计入温度效应与转向传动机构间隙的车辆摆振特性分析

卢剑伟[1]，徐 燚[1]，王锡锌[1]，Stephanos Theodossiades[2]

（1. 合肥工业大学机械与汽车工程学院，合肥 230009； 2. 拉夫堡大学 Wolfson 机械与制造工程学院，拉夫堡 LE113TU）

摘 要：为改善车辆不同作业环境下的操控性能，防止地域及季节气温差异导致转向系动态响应偏离其设计初衷，该文以非独立悬架车辆为例，对考虑温度效应的车辆摆振系统动力学行为进行了分析。基于热弹性力学考察了温度效应对转动副间隙的影响，建立了计入温度效应的转向传动机构含间隙车辆摆振系统动力学模型。通过数值算例分析了某 1030 货车摆振响应的分岔特性和初值特性，讨论了车速、温度等参数对摆振系统全局动力学行为的影响，研究表明，温度的改变在 85～110 km/h 车速区间内会导致转向轮摆角周期运动形态的改变，且这种影响在高车速区段下比中低车速区段更为明显，而当车速为 100 km/h、温度为-40℃时左转向轮摆角中值为负，意味着有向右跑偏趋势；50℃时摆角中值由负变正，说明有改为向左跑偏的趋势。研究结果可为全天候车辆防摆振设计提供参考。

关键词：车辆，温度效应，动力学，间隙，摆振

doi：10.3969/j.issn.1002-6819.2013.14.010

中图分类号：TH132 **文献标志码**：A **文章编号**：1002-6819(2013)-14-0074-08

卢剑伟，徐 燚，王锡锌，等. 计入温度效应与转向传动机构间隙的车辆摆振特性分析[J]. 农业工程学报，2013，29(14)：74－81.

Lu Jianwei, Xu Yi, Wang Xixin, et al. Analysis of shimmy characteristic based on temperature effects and steering linkage clearance for vehicle[J]. Transactions of the Chinese Society of Agricultural Engineering (Transactions of the CSAE), 2013, 29(14): 74－81. (in Chinese with English abstract)

0 引 言

车辆是现代农业广泛应用的机动作业装备，在农业生产及运输环节中担负着重要角色，确保其安全稳定运行是对其基本要求。而摆振是车辆运行中较为常见的一种现象，表现为在良好路面上直线行驶时，由外激励或转向系参数引起的转向轮绕主销摆动、前桥绕纵轴摆动及整车横向运动等[1-20]。摆振影响车辆操控性能，威胁行车安全，因此人们一直力图掌握摆振的发生机理并有效应对[21-28]。尤其近十几年来，计算机和非线性科学的发展使得摆振研究也深入到非线性领域。例如：Kimura 利用试验和数值仿真研究了轻卡的自激摆振[1]；Demic 考虑转向系和悬架的耦合，分析了转向系参数对重卡前轮摆振的影响[2]；Stépán 等利用分岔理论考察了系统参数对前轮摆振响应稳定性的影响[3-4]；作者所在团队围绕间隙主导的车辆摆振系统动力学建模分析也开展了一些工作[5-6,21]。

上述研究在解释车辆摆振发生机理方面取得了很大进展，但仍有不足，研究均以室温工况为前提，而车辆实际作业环境温度差异很大，最低可达-40℃以下，而最高可达 50℃。温度变化导致转向系运动副部件间隙改变，致使车辆转向系统动态响应偏离设计目标，因此有必要对考虑温度效应的车辆摆振系统动力学响应进行深入研究。

基于以上考虑，本文建立计入温度效应的转向传动机构的车辆摆振系统动力学模型，通过系统分岔特性和初值特性分析，评估初始状态及温度等参数对其全局动力学行为的影响。

1 计入温度效应的转动副建模

含间隙转动副如图 1 所示。依据 Hertz 理论，运动副接触状态下 2 个构件作用力与其表面力学性质有关[22]。假设一个构件表面有弹性和摩擦，另一构件为刚体，接触点法向和切向力为

$$P_n = K\delta_n + C_n v_n \quad (1)$$

$$P_t = -f_m \delta P_{21}^n - C_t v_t \quad (2)$$

式中，P_n，P_t 为接触点法向和切向力，N；K 为接触刚度，N/m，通常由试验测试得出，本文中参考文献[21]取值；δ_n 为法向变形，m；C_n，C_t 为法向和切向阻尼系数，N·m/s；P_{21}^n 为轴套对轴销的沿 O_1O_2 方向的法向作用力，N；v_n，v_t 为接触点法向和切

收稿日期：2012-07-10 修订日期：2013-05-14

基金项目：国家自然科学基金（50975071）、教育部新世纪优秀人才支持计划（NCET-10-0358）、常州市应用基础研究计划项目（CJ20110006）。

作者简介：卢剑伟（1975－），男，山东青州人，教授、博士生导师，主要从事车辆动力学相关研究。合肥 合肥工业大学机械与汽车工程学院，230009。Email：jwlu75@163.com

向相对速度，km/h；f_m为摩擦系数；δ 为 v_t方向的符号函数，$\delta=\mathrm{sign}(v_t)=\begin{cases}1 & v_t\geq 0\\ -1 & v_t<0\end{cases}$。

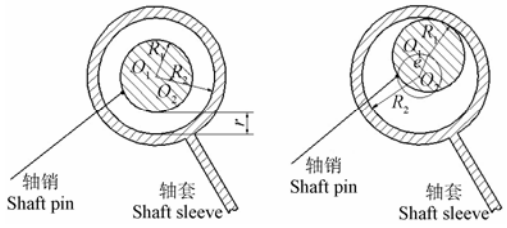

a. 分离状态　　b. 接触状态
a. In separated state　　b. In contact state

注：R_1、R_2为轴销和轴套半径，m；r 为间隙，μm；e 为轴销和轴套中心 O_1O_2 距离，m。
Note: R_1 is the radius of the shaft pin, m; R_2 is the radius of the shaft sleeve, m; r is the clearance, μm; e is the distance between the centers of the shaft pin O_1 and the shaft sleeve O_2, m.

图 1　含间隙转动副示意图

Fig.1　Revolute movement pair with clearance

假定转动副处于稳定的温度场，温度变化导致的变形可通过热弹性力学计算得到。分析时转动副可简化为轴和孔，如图 2。

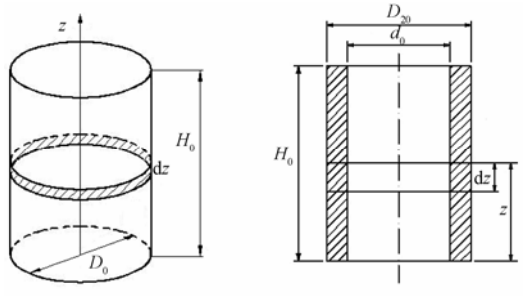

a. 轴类零件　　b. 孔类零件
a. Shaft like component　　b. Hole like component

注：D_0，H_0为轴变形前直径和长度，m；z 为轴线长度，m；d_0，D_{20}为孔变形前内外径，m。
Note: D_0 is the diameter of shaft before deformation, m; H_0 is the length of shaft before deformation, m; z is the length of axis, m; d_0 is the inner diameter of hole before deformation, m; D_{20} is the outside diameter of hole before deformation, m.

图 2　轴、孔类零件示意图

Fig.2　Shaft and hole like components

温度效应引起的轴孔类零件变形主要包括弹性模量变化引起的变形和材料热膨胀引起的变形 2 部分[29-30]，下面分别讨论。

2.1　弹性模量变化引起的变形

轴上微段 dz 承受的垂直载荷 F_Z（N）为[29]

$$F_Z=(H_0-z)D_0^2\cdot\pi\rho g/4 \tag{3}$$

式中，D_0、H_0为轴变形前直径和长度，m；ρ 为材料密度，kg/m^3，则轴上微段 dz(m)的变形量为

$$\mathrm{d}\Delta H_1=\frac{4F_Z}{\pi ED_0^2}\mathrm{d}z \tag{4}$$

式中，E 为随温度变化的弹性模量，MPa，且

$$E=E_0\left(1+\alpha_E\Delta T\right) \tag{5}$$

式中，α_E为材料弹性模量温度系数，℃；E_0为初始弹性模量，MPa；ΔT 为温度变化，℃。

对式（4）积分得整个轴在 z 方向的变形量

$$\Delta H_1=\frac{\rho gH_0^2}{2E_0(1+\alpha_E\cdot\Delta T)} \tag{6}$$

由于 $\alpha_E\Delta T<<1$[29]，式（6）可改写为

$$\Delta H_1=\frac{\rho gH_0^2}{2E_0}\left(1-\alpha_E\Delta T\right) \tag{7}$$

2.2　材料热膨胀引起的变形

由于材料热膨胀产生的变形ΔH_2（m）为

$$\Delta H_2=H_0\alpha\cdot\Delta T \tag{8}$$

式中，α 为材料热膨胀系数，℃。长度方向由温度变化引起的变形ΔH（m）为

$$\Delta H=H_0\alpha\Delta T-\frac{\rho gH_0^2}{2E_0}\alpha_E\Delta T \tag{9}$$

由文献[29]可知，温度变化前后轴的体积 V_0、V_1满足

$$\frac{V_1-V_0}{V_0\Delta T}=3\alpha \tag{10}$$

记 $\frac{\rho ga_E}{2E_0}=\varepsilon$，可得到

$$\frac{\Delta D}{D_0}\approx\sqrt{\frac{3\alpha\Delta T+1}{1+\alpha\Delta T}}-1\approx\left(\alpha+\frac{\varepsilon H_0}{2}\right)\Delta T \tag{11}$$

式中，ΔD 为轴直径的变形量，m。

孔类零件分析过程类似，不再赘述，内径变化为

$$\Delta d=\sqrt{\frac{D_{20}^2\xi^3-D_{20}^2\xi^2\varepsilon H_0\Delta T-\left(1+3\alpha\Delta T\right)\left(D_{20}^2-d_0^2\right)}{\xi-\varepsilon H_0\Delta T}}-d_0 \tag{12}$$

式中，$\xi=1+\alpha\cdot\Delta T$。

由此可得转动副间隙的变化量 Δr（μm）为

$$\Delta r=\Delta d-\Delta D=\Delta d-\left(2\alpha+\varepsilon H_0\right)R_1\Delta T \tag{13}$$

2　计入温度效应的摆振系统模型

以非独立悬架车辆为例，假定横拉杆和左梯形臂之间转动副存在间隙，计及前轮与前桥耦合振动。因为要考察的摆振工况系自激振动，因此路面不平激励可忽略，方向盘保持直线行驶状态，得到摆振系统模型如图 3。

参考文献[5-6]中转向机构的受力分析，可得到作用于转向节的力矩分别为

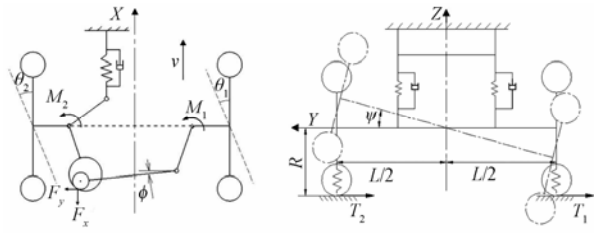

a. 俯视图 b. 后视图
a. Plan view b. Rear view

注：θ_2，θ_1 为左右轮摆角，rad；ψ 为前桥绕纵轴摆角，rad；ϕ为横拉杆摆角，rad；M_2，M_1 为左右转向节上的力矩，N·m；T_2，T_1 为左右轮胎侧偏力，N；R 为轮胎半径，m；v 为车速，km/h；F_x，F_y 为接触力在 XY 方向的分力，N。
Note: θ_1 is the shimmy angle of right front wheel, rad; θ_2 is the shimmy angle of left front wheel, rad; ψ is rolling angle of front axle, rad; ϕ is the shimmy angle of tie-rod, rad; M_1 is the moment applied on the right steering knuckle, N·m; M_2 is the moment applied on the left steering knuckle, N·m; T_1 is the side force of right front wheel, N; T_2 is the side force of left front wheel, N; R is the radius of the wheel, m; v is the vehicle velocity, km/h; F_x is the contact component force in the X direction, N; F_y is the contact component force in the Y direction, N.

图 3 摆振系统模型示意图

Fig.3 Diagram of vehicle shimmy system

$$\begin{aligned}M_1=\{&-m_1[\left(\frac{\mathrm{d}\theta_1}{\mathrm{d}t}\right)^2\cos(\theta_1+\Phi)l_1+\\&\frac{\mathrm{d}^2\theta_1}{\mathrm{d}t^2}l_1\sin(\theta_1+\Phi)+\frac{\mathrm{d}^2\phi}{\mathrm{d}t^2}\frac{l_{ram}}{2}\sin\phi+\\&\left(\frac{\mathrm{d}\phi}{\mathrm{d}t}\right)^2\frac{l_{ram}}{2}\cos\phi]+F_x\}\ \sin(\theta_1+\Phi)l_1-\\&\{m_1[\left(\frac{\mathrm{d}\theta_1}{\mathrm{d}t}\right)^2 l_1\sin(\theta_1+\Phi)+\\&\frac{\mathrm{d}^2\theta_1}{\mathrm{d}t^2}l_1\cos(\theta_1+\Phi)\ +\frac{\mathrm{d}^2\phi}{\mathrm{d}t^2}\frac{l_{ram}}{2}\cos\phi+\\&\left(\frac{\mathrm{d}\phi}{\mathrm{d}t}\right)^2\frac{l_{ram}}{2}\sin\phi]+F_y\}l_1\cos(\theta_1+\Phi)\end{aligned}\tag{14}$$

$$\begin{aligned}M_2=&[F_y\cos(\pi-\Phi+\theta_2)-F_x\sin(\pi-\Phi+\\&\theta_2)]l_2+(F_y\cos\beta-F_x\sin\beta)R_1+(F_y\mathrm{e}_x-F_x\mathrm{e}_y)\end{aligned}\tag{15}$$

式中，t 为时间，s；Φ 为转向梯形底角，(°)；m_1 为右梯形臂质量，kg；l_2、l_1 为左右梯形臂长度，m；l_{ram} 为横拉杆长度，m；e_x、e_y 为 e 在 XY 方向分量，μm；β 为 O_1O_2 与 X 轴夹角，(°)；$\frac{\mathrm{d}\theta_1}{\mathrm{d}t}$ 为右轮绕主销的摆角速度，rad/s；$\frac{\mathrm{d}\phi}{\mathrm{d}t}$ 为横拉杆摆角速度，rad/s。

接触力在 XY 方向的分力 F_x、F_y 与接触点法向和切向力 P_n、P_t 的关系为

$$\begin{cases}F_x=P_n\cos\beta-P_t\sin\beta\\F_y=P_n\sin\beta+P_t\cos\beta\end{cases}\tag{16}$$

由此，得出右轮绕主销运动方程为

$$\begin{aligned}&I_1\frac{\mathrm{d}^2\theta_1}{\mathrm{d}t^2}+c_4\frac{\mathrm{d}\theta_1}{\mathrm{d}t}+I_2\frac{v}{R}\frac{\mathrm{d}\psi}{\mathrm{d}t}-[\frac{L}{2}k_5l(\gamma-f)+\\&k_4R^2\gamma]\psi+T_1(R\gamma+\beta)-M_1=0\end{aligned}\tag{17}$$

左轮绕主销运动方程为

$$\begin{aligned}&I_1\frac{\mathrm{d}^2\theta_2}{\mathrm{d}t^2}+(c_2+c_4)\frac{\mathrm{d}\theta_2}{\mathrm{d}t}+k_2\theta_2+I_2\frac{v}{R}\frac{\mathrm{d}\psi}{\mathrm{d}t}-\\&[\frac{L}{2}k_5l(\gamma-f)+k_4R^2\gamma]\psi+T_2(R\gamma+\beta)-M_2=0\end{aligned}\tag{18}$$

前桥侧摆运动方程为

$$\begin{aligned}&I_3\frac{\mathrm{d}^2\psi}{\mathrm{d}t^2}-c_3\frac{\mathrm{d}\psi}{\mathrm{d}t}+[k_3+\frac{L^2}{2}k_5+2k_4R^2]\psi-\\&I_2\frac{v}{R}(\frac{\mathrm{d}\theta_1}{\mathrm{d}t}+\frac{\mathrm{d}\theta_2}{\mathrm{d}t})-(T_1+T_2)R_1=0\end{aligned}\tag{19}$$

横拉杆横摆运动方程为

$$\begin{aligned}&I_{ram}\frac{\mathrm{d}^2\phi}{\mathrm{d}t^2}-(F_x\sin\phi-F_y\cos\phi)l_{ram}-(F_x\sin\beta-\\&F_y\cos\beta)R_1+m_1\frac{l_{ram}}{2}[\frac{\mathrm{d}^2\theta_1}{\mathrm{d}t^2}l_1\cos(\theta_1+\Phi-\phi)-\\&\left(\frac{\mathrm{d}\theta_1}{\mathrm{d}t}\right)^2 l_1\sin(\theta_1-\phi)]=0\end{aligned}\tag{20}$$

式中，I_1、I_2 分别为车轮绕主销及自身旋转轴线的转动惯量，kg·m^2；I_3 为前桥绕其纵轴线转动惯量，kg·m^2；I_{ram} 为横拉杆绕经过质心垂线的转动惯量，kg·m^2；$\frac{\mathrm{d}\psi}{\mathrm{d}t}$ 为前桥绕纵轴摆角速度，rad/s；$\frac{\mathrm{d}\theta_2}{\mathrm{d}t}$ 为左轮绕主销的摆角速度，rad/s；c_4 为车轮绕主销当量阻尼，N·s/m；k_4、k_5 为轮胎侧向和垂向刚度，kN/m；γ 为主销后倾角，rad；f 为滚动阻力系数；l 为主销延长线与地面交点到车轮对称面距离，m；L 为轮距，m；c_2 为换算到主销的直拉杆阻尼，N·s/m；k_2 为换算到主销的直拉杆刚度，kN/m；c_3 为换算到前桥侧摆中心的悬架当量角阻尼，N·s/(m·rad)；k_3 为换算到前桥侧摆中心的悬架当量角刚度，kN/(m·rad)。

根据 Pacejka 提出的“魔术公式”轮胎模型，轮胎侧偏力定义如下[32]

$$\begin{cases}T_1=S_y+U\sin\{C\arctan[B(\alpha_1-S_x)(1-A)+\\A\arctan B(\alpha_1-S_x)]\}\\T_2=S_y+U\sin\{C\arctan[B(\alpha_2-S_x)(1-A)+\\A\arctan B(\alpha_2-S_x)]\}\end{cases}\tag{21}$$

式中，α_2、α_1 为左右车轮侧偏角，rad；常系数 S_x、S_y、A、B、C、U 由试验结果拟合得到，文中参考文献[6]确定。

根据张线理论[32]，侧偏角与车轮摆角间约束为

$$\begin{cases}\frac{\mathrm{d}\alpha_1}{\mathrm{d}t}+\frac{v}{\sigma}\alpha_1+\frac{v}{\sigma}\theta_1-\frac{a}{\sigma}\frac{\mathrm{d}\theta_1}{\mathrm{d}t}=0\\\frac{\mathrm{d}\alpha_2}{\mathrm{d}t}+\frac{v}{\sigma}\alpha_2+\frac{v}{\sigma}\theta_2-\frac{a}{\sigma}\frac{\mathrm{d}\theta_2}{\mathrm{d}t}=0\end{cases}\tag{22}$$

式中，σ 为轮胎松弛长度，m；$\frac{\mathrm{d}\alpha_2}{\mathrm{d}t}$、$\frac{\mathrm{d}\alpha_1}{\mathrm{d}t}$ 为左右

车轮侧偏角速度，rad/s。将式（16）～式（22）转化为一阶标准型微分方程组

$$\begin{cases}
\dfrac{\mathrm{d}x_1}{\mathrm{d}t}=x_2\\
\dfrac{\mathrm{d}x_2}{\mathrm{d}t}=[I_{ram}(P+Q)-m_1l_1\dfrac{l_{ram}}{2}\cos(\theta_1+\\
\Phi-\phi)]W/[I_{ram}(I_1+m_1l_1^2)-\\
(m_1l_1\dfrac{l_{ram}}{2})^2\cos^2(\theta_1+\Phi-\phi)]\\
\dfrac{\mathrm{d}x_3}{\mathrm{d}t}=x_4\\
\dfrac{\mathrm{d}x_4}{\mathrm{d}t}=-\dfrac{(c_2+c_4)}{I_1}x_4-\dfrac{k_2}{I_1}x_3-\\
\dfrac{I_2}{I_1}\dfrac{v}{R}x_6+\dfrac{1}{I_1}[\dfrac{L}{2}k_5l(\gamma-f)+\\
k_4R^2\gamma]x_7-\dfrac{T_2}{I_1}(R\gamma+\beta)+\dfrac{M_2}{I_1}\\
\dfrac{\mathrm{d}x_5}{\mathrm{d}t}=x_6\\
\dfrac{\mathrm{d}x_6}{\mathrm{d}t}=-\dfrac{c_3}{I_3}x_6-\dfrac{1}{I_3}[k_3+\dfrac{L^2}{2}k_5+2k_4R^2]x_5+\\
\dfrac{I_2}{I_3}\dfrac{v}{R}(\dfrac{\mathrm{d}\theta_1}{\mathrm{d}t}+\dfrac{\mathrm{d}\theta_2}{\mathrm{d}t})+(T_1+T_2)\dfrac{R_1}{I_3}\\
\dfrac{\mathrm{d}x_7}{\mathrm{d}t}=x_8\\
\dfrac{\mathrm{d}x_8}{\mathrm{d}t}=(F_x\sin x_7-F_y\cos x_7)\dfrac{l_{ram}}{I_{ram}}+\\
(F_x\sin\beta-F_y\cos\beta)\dfrac{R_1}{I_{ram}}-\\
m_1\dfrac{l_{ram}}{2I_{ram}}[\dfrac{\mathrm{d}x_2}{\mathrm{d}t}l_1\cos(\theta_1+\Phi-\phi)\ -\\
x_2^2l_1\sin(\theta_1+\Phi-\phi)]\\
\dfrac{\mathrm{d}x_9}{\mathrm{d}t}=-\dfrac{v}{\sigma}x_7-\dfrac{v}{\sigma}x_1+\dfrac{a}{\sigma}x_2\\
\dfrac{\mathrm{d}x_{10}}{\mathrm{d}t}=-\dfrac{v}{\sigma}x_8-\dfrac{v}{\sigma}x_3+\dfrac{a}{\sigma}x_4
\end{cases}\tag{23}$$

$$P=-c_4\frac{\mathrm{d}\theta_1}{\mathrm{d}t}-I_2\frac{v}{R}\frac{\mathrm{d}\psi}{\mathrm{d}t}+[\frac{L}{2}k_5l(\gamma-f)+k_4R^2\gamma]\psi-T_1(R\gamma+\beta)\tag{24}$$

$$Q=-[m_1l_1^2\sin(2\theta_1+2\Phi)\left(\frac{\mathrm{d}\theta_1}{\mathrm{d}t}\right)^2+m_1l_1\frac{l_{ram}}{2}\sin(\theta_1+\Phi+\phi)\cdot\left(\frac{\mathrm{d}\phi}{\mathrm{d}t}\right)^2]+F_xl_1\sin(\theta_1+\Phi+\phi)-F_yl_1\cos(\theta_1+\Phi)\tag{25}$$

$$W=m_1l_1\frac{l_{ram}}{2}\sin(\theta_1+\Phi-\phi)\left(\frac{\mathrm{d}\theta_1}{\mathrm{d}t}\right)^2+l_{ram}(F_x\sin\phi-F_y\cos\phi)+R_1(F_x\sin\beta-F_y\cos\beta)\tag{26}$$

车速 v 对摆振影响较大，转向系统工艺参数设计以室温 20℃为前提，故将当前温度 T=20+ΔT 也视为状态变量，系统状态方程可表示为

$$\frac{\mathrm{d}x}{\mathrm{d}t}=f(x,v,T)\tag{27}$$

式中，$x=\left(\theta_1,\dfrac{\mathrm{d}\theta_1}{\mathrm{d}t},\theta_2,\dfrac{\mathrm{d}\theta_2}{\mathrm{d}t},\psi,\dfrac{\mathrm{d}\psi}{\mathrm{d}t},\phi,\dfrac{\mathrm{d}\phi}{\mathrm{d}t},\alpha_1,\alpha_2\right)^T=(x_1,x_2,x_3,x_4,x_5,x_6,x_7,x_8,x_9,x_{10})^T$ 为状态变量。

3　数值分析

基于上述模型，分析温度对某 1030 货车摆振系统响应的影响。假设右转向轮受偶发激励有很小的初速度 0.01 rad/s，室温下运动副间隙为 r=50 μm，通过算例考察温度改变时摆振系统的响应，其它系统结构参数如表 1。

表 1　系统结构参数列表

Table 1　System parameters for numerical analysis

参数 Parameter	数值 Value	参数 Parameter	数值 Value
车轮绕主销的转动惯量 I_1/(kg·m^2)	6.0	换算到主销横拉杆阻尼 c_1/(kN·s·m^{-1})	100
车轮绕自身转轴转动惯量 I_2/(kg·m^2)	4.85	换算到主销转向机构等效阻尼 c_3/(kN·m·s·rad^{-1})	1.05e3
前桥绕纵轴转动惯量 I_3/(kg·m^2)	160	换算到前桥侧摆中心悬架角阻尼 c_4/(kN·s·m^{-1})	44
横拉杆绕销轴转动惯量 I_{ram}/(kg·m^2)	1.415	横拉杆质量 m_1/kg	6.5
换算到主销横拉杆刚度 k_1/(kN·m^{-1})	35.5	间隙副轴销半径 R_1/m	0.018
换算到前桥侧摆中心悬架角刚度 k_3/(kN·m^{-1}·rad^{-1})	32	转向梯形底角 Φ/(°)	70
轮胎侧向刚度 k_4/(kN·m^{-1})	80	轮距 L/m	1.608
轮胎垂向刚度 k_5/(kN·m^{-1})	400	轮胎松弛长度 σ/m	0.65
横拉杆长度 l_{ram}/m	1.3474	轮胎半径 R/m	0.4
梯形臂长度 l_1/m	0.015	主销后倾角 γ/rad	0.04

选择低挡和高档运行时 2 个常用车速 32 和 80 km/h 进行分析，得到转向轮摆角随温度变化情况如图 4。从图 4 中看出：其它参数保持不变、只有温度改变时，转向轮摆角响应的周期运动特征保持稳定，即单纯温度变化一般不会改变摆振系统响应的运动形态；但转向轮摆角幅值会随着温度上升而减小。

分别选择极低温度-40℃和极高温度 50℃两种工况，考察转向轮摆角响应随车速变化的分岔

特性[27]，结果如图 5。从图 5 中看出：温度改变对右转向轮摆角响应影响很小，而主要体现为对左转向轮的影响，这与本文仅考虑左梯形臂与横拉杆之间的间隙有关。说明温度变化对含间隙机构动态响应的影响不容忽视；同时，温度对左转向轮的影响主要体现在高车速区段，而在中低车速区段影响较小，在 85～110 km/h 的高车速区段运行时，环境温度变化会导致其左转向轮摆角周期特性发生明显改变。

图 6 是-40℃和 50℃、车速为 100 km/h 时左转向轮响应。从图中可以看出：给定 2 种温度工况下，左转向轮响应的周期运动特征没有变化，但其相轨迹已明显改变。从时间历程分析结果可以发现：与常温工况下转向轮摆角响应中值为 0 不同，-40℃时左转向轮摆角响应中值为负值，且数值较小，意味着左转向轮会向右轻度跑偏；而 50℃时左转向轮摆角响应中值由负变正，意味着跑偏方向改变为向左轻度跑偏。

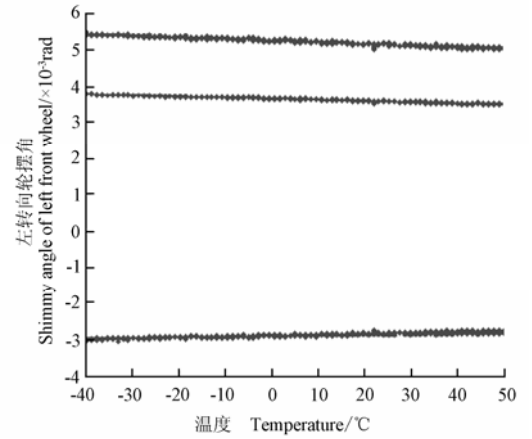

a. 左转向轮（v=32 km/h）
a. Left front wheel (v=32 km/h)

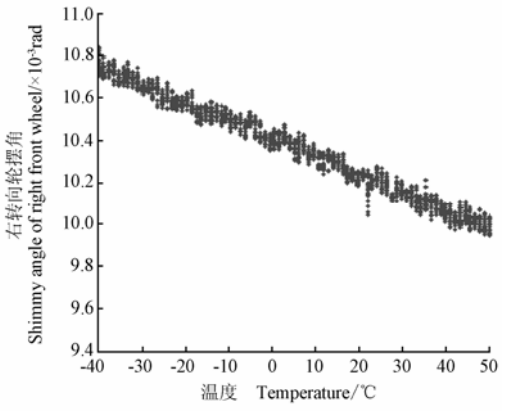

b. 右转向轮（v=32 km/h）
b. Right front wheel (v=32 km/h)

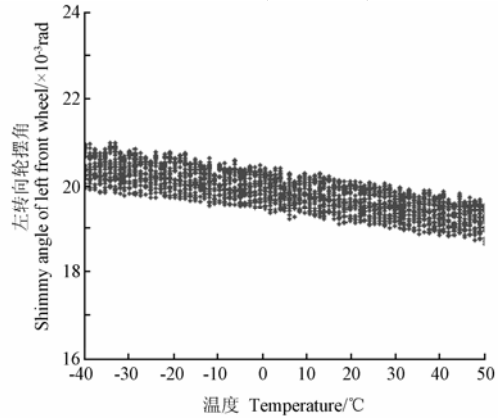

c. 左转向轮（v=80 km/h）
c. Left front wheel (v=80 km/h)

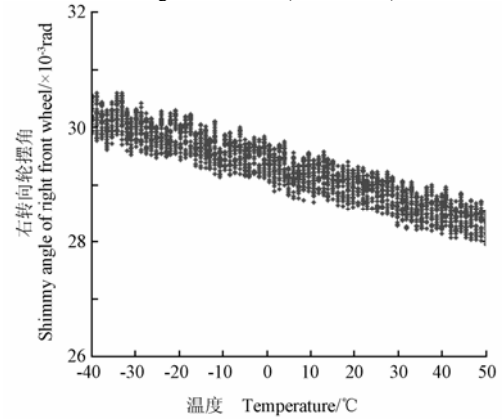

d. 右转向轮（v=80 km/h）
d. Right front wheel (v=80 km/h)

注：间隙 r=50 μm。
Note: clearance r=50 μm.

图 4 不同车速下转向轮摆角随温度变化

Fig.4 Variation of shimmy angles of front wheels under different vehicle speed

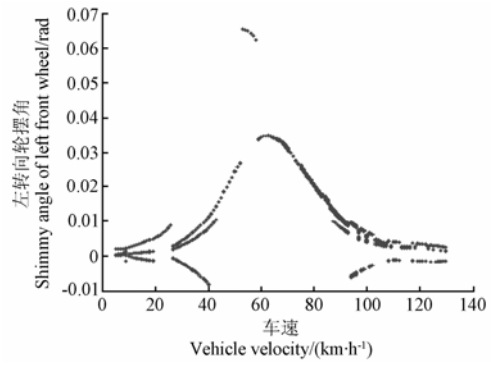

a. 左转向轮（温度 T=-40℃）
a. Left front wheel(T=-40℃)

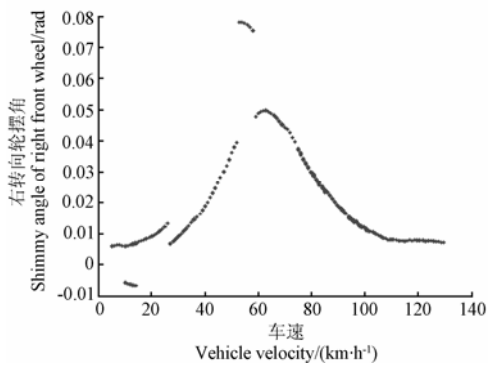

b. 右转向轮（温度 T=-40℃）
b. Right front wheel(T=-40℃)

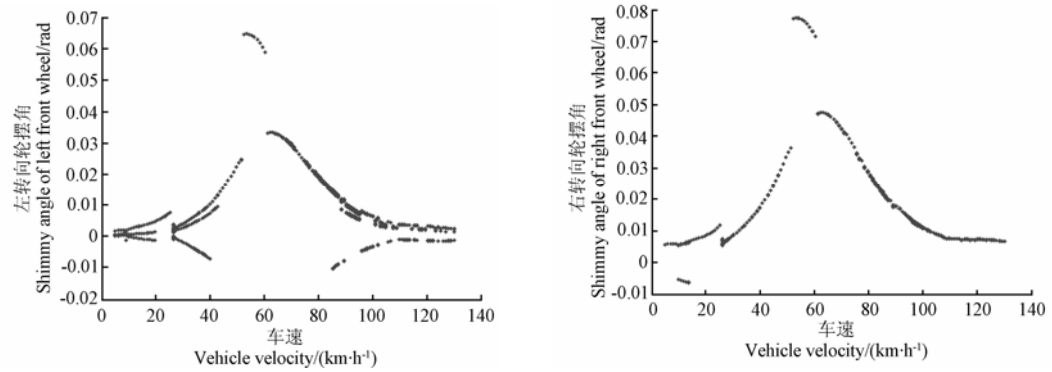

c. 左转向轮(温度 T=50℃)　　d. 右转向轮(温度 T=50℃)
c. Left front wheel(T=50℃)　　d. Right front wheel(T=50℃)

图 5　极限温度下转向轮摆角随车速变化的分岔图

Fig.5　Bifurcation of shimmy angles of front wheels with variation of vehicle speed under limit temperature

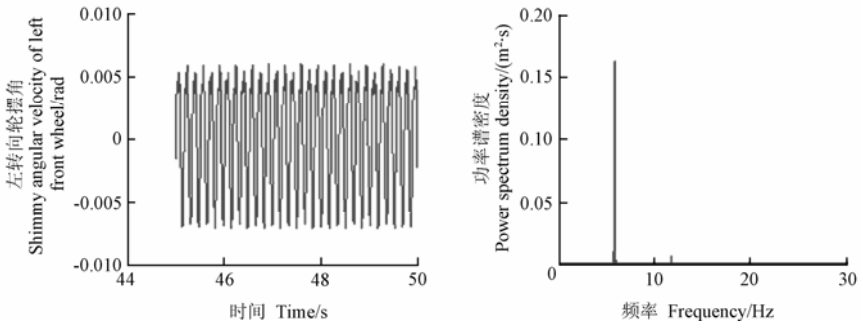

a. 时间历程(T= -40℃)　　b. 功率谱图(T= -40℃)
a. Time history(T= -40℃)　　b. Power spectrum density(T= -40℃)

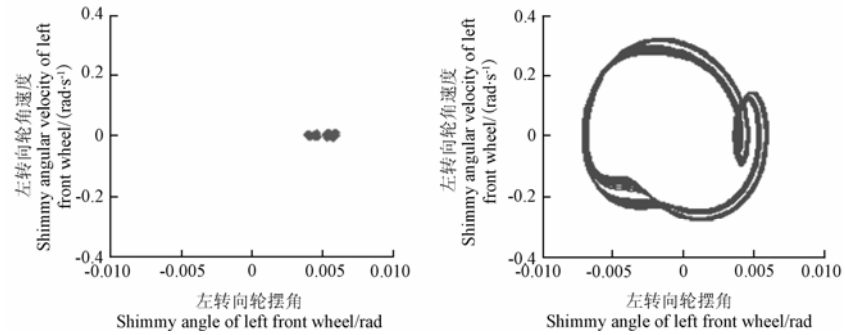

c. Poincare 映射(T= -40℃)　　d. 相图(T= -40℃)
c. Poincare mapping(T= -40℃)　　d. Phase portrait(T= -40℃)

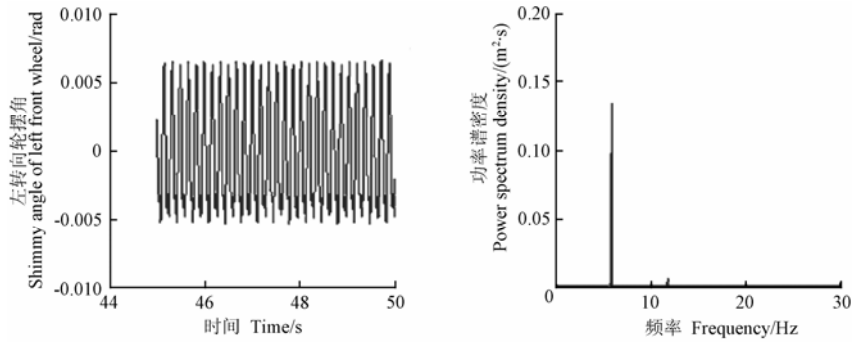

e. 时间历程(T=50℃)　　f. 功率谱图(T=50℃)
e. Time history(T=50℃)　　f. Power spectrum density(T=50℃)

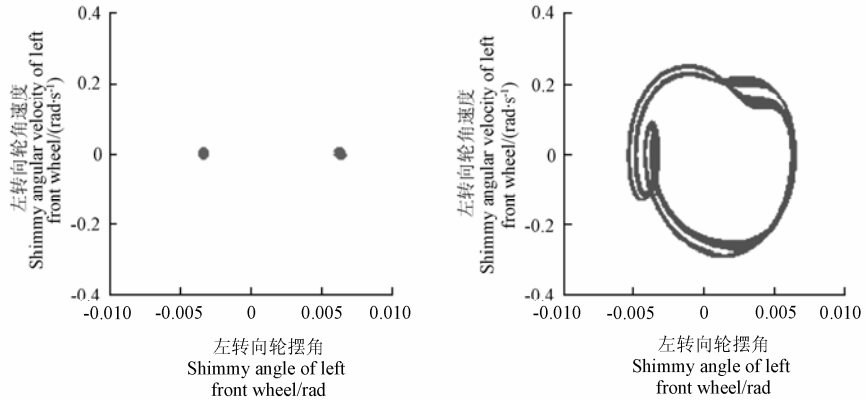

g. Poincare 映射(T=50℃)
g. Poincare mapping(T=50℃)

h. 相图(T=50℃)
h. Phase portrait(T=50℃)

注：车速 v=100 km/h。
Note: Vehicle speed v=100 km/h。

图 6 极限温度下左转向轮响应

Fig.6 Response of left front wheel under limit temperature

4 结 论

1）温度的改变在某些工况下会导致含间隙转向传动机构的车辆摆振系统动力学行为发生改变，因此在摆振系统动力学分析中考虑温度的影响是有必要的。

2）温度对于车辆摆振系统的影响与车速有关。本文所研究的 1030 货车在 85～110 km/h 车速区间内，温度变化会导致左转向轮摆角周期特性发生改变，而在中低车速区段 20～65 km/h 车速区间，温度对其影响不明显。

3）文中建模时仅考虑左梯形臂与横拉杆间的间隙，因此温度对车辆摆振影响主要体现为左转向轮动力学行为的变化，而对右转向轮影响很小。当车速为 100 km/h、温度为-40℃时左转向轮摆角中值为负值，意味着有向右跑偏的趋势；而 50℃时摆角中值由负变正，有改为向左跑偏的趋势。

4）车速、间隙等其它工况参数不变前提下，单纯温度变化一般不会改变摆振系统响应的运动形态，但转向轮摆角幅值会随着温度上升而减小。

[参 考 文 献]

[1] Kimura T, Hanamura Y. Analysis of steering shimmy accompanied by sprung mass vibration on light duty truck-fundamental mechanism[J]. ISAE Review, 1996, 17(3): 301－306.

[2] Demic M. Analysis of influence of design parameters on steered wheels shimmy of heavy vehicle[J]. Vehicle System Dynamic, 1996, 26(5): 343－362.

[3] Takacs D, Stépán G., Hogan S J. Isolated large amplitude periodic motions of towed rigid wheels[J]. Nonlinear Dynamics, 2008, 52(1/2): 27－34.

[4] Takacs D, Stépán G. Experiments on quasi- periodic wheel shimmy[C]// ASME IDETC/CIE 2007, Las Vegas, Nevada, 2007.

[5] Lu Jianwei, Gu Jue, Liu Mengjun. Modeling of the vehicle shimmy system with consideration of clearance of the steering mechanism[J]. Meccanica, 2010, 45(1): 53－61.

[6] Lu J W, Xin J Y, Lee J K. Dynamic behavior analysis of vehicle shimmy system with consideration of clearance in steering linkage mechanism[C]// ASME DETC2012-70215, 2012.

[7] Kim K W, Park J B. Tire mass imbalance, rolling phase difference, and inflation pressure change effects on steering wheel vibration[C]// SAE Paper 2005-01-2317.

[8] Meyers A. The development of non-hydraulic shimmy dampers[C]// SAE Paper 2000-01-1710.

[9] Sugiyama A, Kurishige M, Hamada H. An EPS control strategy to reduce steering vibration associated with disturbance from road wheels[C]// SAE Paper 2006-01-1178.

[10] Demers M A. Steering wheel vibration diagnosis[C]// SAE Paper 2001-01-1607.

[11] Takács D, Stépán G. Experimental modal analysis of towed elastic tyres during rolling[M]. Springer Press, 2010.

[12] Shaw S W, Balachandran B. A review of nonlinear dynamics of mechanical systems in year 2008[J]. Journal of System Design and Dynamics, 2008, 2(3): 611－640.

[13] Sharp R S, Evangelou S. Advances in the modeling of motorcycle dynamics[J]. Multibody System Dynamics, 2004, 12(3): 251－283.

[14] Takacs D, Stépán G. Dynamic contact problem of rolling elastic wheels[C]// Proceedings of ICGF 2006.

[15] Dénes T, Gábor O, Gábor S. Delay effects in shimmy dynamics of wheels with stretched string-like tyres[J]. European Journal of Mechanics-A/Solids, 2009, 28(3): 516－525.

[16] 林逸，李胜. 非独立悬架汽车转向轮自激型摆振的分岔特性分析[J]. 机械工程学报，2004，40(12)：187－191.
Lin Yi, Li Sheng. Study on the bifurcation character of steering wheel self-excited shimmy of motor vehicle with dependent suspension[J]. Chinese Journal of Mechanical Engineering, 2004, 40(12): 187－191. (in Chinese with English abstract)

[17] Ayglon V. Experimental testing and validation of tangential steering wheel vibrations due to tire nonuniform[J]. ASME Dynamic Systems and Control Division, 2005, 74(1): 545－551.

[18] Popp K, Schiehlen W. Ground vehicle dynamics[M]. Berlin: Springer press, 2012.

[19] Mcwilliams J, Bleitzd W. Steering grunt noise robustness improvement[C]// SAE Paper 2009-01-2095.

[20] Zhuravlev V P, Klimov D M. The causes of the shimmy phenomenon[J]. Doklady Physics, 2009, 54(10): 475－478.

[21] 卢剑伟，顾驶. 运动副间隙对汽车摆振系统非线性动力学行为影响分析[J]. 机械工程学报，2008，44(8)：

169－173.
Lu Jianwei, Gu Jue. Influence analysis of movement pair clearance on nonlinear dynamic behavior of vehicle shimmy system[J]. Chinese Journal of Mechanical Engineering, 2008, 44(8): 169－173. (in Chinese with English abstract)
[22] Jinghong Yu, Brian Brickner. Analysis of Vehicle Chassis Transmissibility of Steering Shimmy and Brake Judder: Mechanism Study and Virtual Design of Experiment[C]// SAE Paper 2007-01-2342.
[23] Gordon J T. Perturbation analysis of nonlinear wheel shimmy[J]. Journal of Aircraft, 2002, 39(2): 305－317.
[24] Jinghong Yu, Brian Nutwell. Analysis of Vehicle Chassis Transmissibility of Steering Shimmy and Brake Judder: System Modeling and Validation[C]// SAE Paper 2007 -01-2341
[25] 刘延柱，陈立群. 非线性振动[M]. 北京：高等教育出版社，2001
[26] Dhooge A, Govaerts W, Kuznetsov Yu A. Matcont: A MATLAB package for numerical bifurcation analysis of ODEs[J]. Journal of ACM Transactions on Mathematical Software, 2003, 29(2): 141－164.
[27] 丁文镜. 自激振动[M]. 北京：清华大学出版社，2009.
[28] Fernholz C M, Nessler G L. Prediction of vehicle steering system NVH from component-level test data[C]// SAE Paper 2006-01-0483.
[29] 费业泰. 机械热变形理论及应用[M]. 北京：国防工业出版社，2009.
[30] Bing S, Ye J. Dynamic analysis of the reheat-stop-valve mechanism with revolute clearance joint in consideration of thermal effect[J]. Mechanism and Machine Theory, 2008, 43(12): 1625－1638.

Analysis of shimmy characteristic based on temperature effects and steering linkage clearance for vehicle

Lu Jianwei[1], Xu Yi[1], Wang Xixin[1], Stephanos Theodossiades[2]
(1. *School of Mechanical and Automotive Engineering*, *Hefei University of Technology*, *Hefei* 230009, *China*;
2. *Wolfson School of Mechanical and Manufacturing Engineering*, *Loughborough University*, *Loughborough*, *LE*113*TU*, *UK*)

Abstract: Vehicles work in outdoor environments to deliver goods or people, while the ambient temperature varies in different seasons or different regions. Since the process parameters of the kinetic pair in vehicle steering mechanisms are usually designed based on the domestic temperature of 20ºC, the temperature variation usually leads to mechanical deformation of components of kinetic pairs in vehicle steering mechanisms, and as a result, the deformation of the components may change the kinetic and dynamic characters of the kinetic pair. Consequently, the dynamic response of the steering system may vary if the vehicle is exposed to different temperature working conditions. As a result, the dynamic behavior of the vehicle shimmy system may be influenced by the temperature effect. Actually, some cases have been reported that the dynamic response of the steering system of certain vehicles varied in different seasons or in different regions. To evaluate the influence of temperature effects on the dynamic response of the vehicle shimmy system with clearance in the steering mechanism, and to prevent the potential deviation of the dynamic response of the steering system from its original design goal, the dynamic behavior of the vehicle shimmy system with clearance in steering linkage with consideration of temperature effect is discussed. Based on thermal elasticity, thermal deformation of kinetic pair components is calculated, and the influence of temperature effects on clearance of revolute kinetic pair was analyzed. As a result, interaction forces between the kinetic pair components with consideration of temperature effect is re-evaluated, and the sub dynamic model of the kinetic pair with clearance with consideration of temperature effect is available. Consequently, a vehicle with dependent suspension was employed as an example, and the dynamic model of the vehicle shimmy system with clearance in steering linkage with consideration of temperature effect is presented. Based on this model, the dynamic behavior of the vehicle shimmy system with clearance with consideration of temperature effects was discussed. Bifurcation characteristics and initial value characteristics of the system were analyzed with numerical examples, and the coupling influences of the temperature and other system parameters, such as vehicle speed, etc, on the global dynamic behavior of the vehicle shimmy system were evaluated. The results show that the temperature and other parameters can make a significant coupling contribution to the dynamic response of the vehicle shimmy system. The change of ambient temperature may lead to significant variation of the dynamic behavior of the system, and it seems that the influence is likely to be more significant at a higher speed range than that at lower speed range. For those examples presented in the paper, the dynamic behavior of the system is significantly affected by temperatures in the speed range 85km/h~110km/h, while it remains stable in lower speed ranges. The method and conclusions presented in this paper may provide theoretical basis for improvement of a vehicle shimmy control with consideration of temperature effect, and they are helpful to perfect the modeling theory of vehicle shimmy system.
Key words: vehicles, thermal effects, dynamics, clearance, shimmy

（责任编辑：鲍洪杰）